PHYSICAL REVIEW C **90**, 064002 (2014)

Zemach moments of ^{3}He and ^{4}He

Ingo Sick*

Department für Physik, Universität Basel, CH4056 Basel, Switzerland

(Received 9 October 2014; revised manuscript received 17 November 2014; published 11 December 2014)

The world data on elastic electron scattering on ^{3}He and ^{4}He is used to determine the Zemach moments $\langle r\rangle_{(2)}$ and $\langle r^3\rangle_{(2)}$. These quantities are required to interpret the Lamb shift and hyperfine splitting data of muonic helium presently being measured at the Paul Scherrer Institute by the CREMA Collaboration. The rms radii are determined as well.

DOI: 10.1103/PhysRevC.90.064002 PACS number(s): 27.10.+h, 25.30.Bf, 21.10.Ky

I. INTRODUCTION

I present results on the rms radii and Zemach moments of the helium isotopes ^{3}He and ^{4}He. The interest in these integral quantities is threefold:

1. Precise moments are useful observables for the comparison with theoretical calculations. This is true in particular for light nuclei such as the helium isotopes where very accurate *ab initio* calculations can be performed.

2. At present there are experiments underway to measure the charge rms radii of the helium nuclei via the Lamb shift in the muonic helium ion [1]. For the interpretation of these data—which will ultimately provide rms radii that are much more precise than the ones extracted from electron scattering—corrections depending on the Zemach radii are needed [2,3]. These quantities can be determined via electron scattering.

3. There is presently a major discrepancy between the rms radius of the proton as determined from electron scattering [4] and muonic hydrogen [5]. One of the speculations concerning the origin of this discrepancy involves a potential difference in the "electromagnetic" interaction between electrons and muons. It is then desirable to make a comparison between radii from experiments involving e and μ for other cases. The most accurate confrontation can be performed for ^{4}He, the nucleus for which the relative uncertainty of the rms radius from electron scattering is smallest.

Also note that the measurements in the (electronic) helium atom of the ^{3}He-^{4}He isotopic shift differ by several standard deviations. It is of interest to see whether electron scattering can help to resolve the issue.

II. MOMENTS FOR ^{4}He

For the interpretation of the Lamb-shift data for muonic ^{4}He, which are presently being taken by Antognini *et al.* at the Paul Scherrer Institute, the third Zemach moment is needed in order to extract the rms radius. This moment can be computed [2,3] from the charge form factor $G_e(q)$ depending on momentum transfer q, that is,

$$\langle r^3\rangle_{(2)} = \frac{48}{\pi}\int_0^\infty \frac{dq}{q^4}\left[G_e^2(q) - 1 + q^2R^2/3\right],$$

where R is the charge rms radius.

In [6] I performed a sum-of-Gaussians (SOG) fit to the world data on elastic electron scattering from ^{4}He [7–12]. For completeness, I added the recently published high-q data of Camsonne *et al.* [13] and redid the fit. For details see [6]. The resulting charge rms radius is (as in [6]) 1.681 ± 0.004 fm. The third Zemach moment is found to be 16.73 ± 0.10 fm^3, where the error covers both the random and systematic uncertainties of the data. For comparison: for Gaussian (exponential) densities—which are often used to estimate $\langle r^3\rangle_{(2)}$—this moment, for the same rms radius, would amount to 16.50 (17.99) fm^3.

One should note that the appearance of the $1/q^4$ factor in the expression for $\langle r^3\rangle_{(2)}$ does not imply that this moment depends strongly on the (e,e) data at extremely low q. The low-q dependence of $G(q) \sim 1 - q^2R^2/6 + \cdots$ cancels the $-1 + q^2R^2/3$ term. In Fig. 1 I show the convergence of the Zemach integral as a function of the upper integration limit. While the full curve gives the Zemach integral (which converges very slowly), the dashed curve has the integral over the form-factor-independent term $(-1 + q^2R^2/3)/q^4$ up to $q = \infty$ added in. These curves show that the experimental information on $G(q)$ in the entire region 0–1 fm^{-1} contributes; above $q \sim 1.2$ fm^{-1}, $G(q)$ is too small to contribute substantially. The q region of sensitivity to $\langle r^3\rangle_{(2)}$ turns out to be quite similar to the one for the rms radius and the first Zemach moment to be discussed below.

For some applications it might also be useful to have the fourth moment $\langle r^4\rangle$. It amounts to 14.35 ± 0.11 fm^4. The various moments are summarized in Table I.

III. MOMENTS FOR ^{3}He

Since Antognini *et al.* are studying muonic ^{3}He as well, I have performed a similar analysis of the world data for ^{3}He. For this nucleus a less extensive set of data is available [9–12,14–20]. The data are in general not as precise as for ^{4}He. A complication arises from the spin-1/2 nature of ^{3}He. In this case the data depend on *two* quantities, the charge (monopole) and the magnetic (dipole) form factors G_e and G_m, respectively. As both forward- and backward-angle data are available, these form factors can be separated, at the expense of an increase of the uncertainties. Figure 2 shows the low-q data which are of special interest for the determination of the moments.

*ingo.sick@unibas.ch

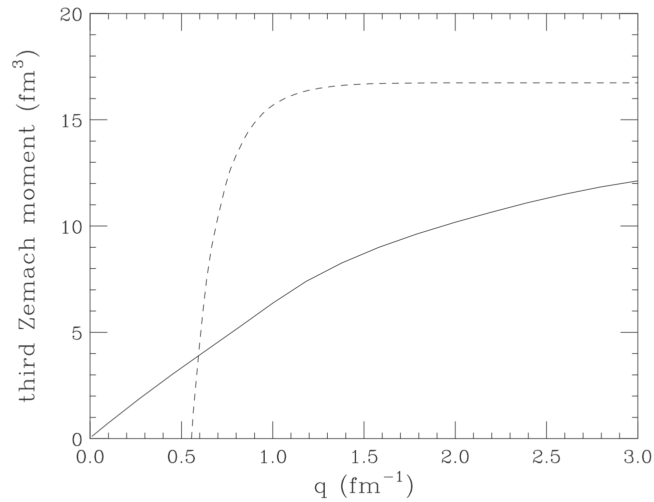

FIG. 1. Convergence of the integral for $\langle r^3\rangle_{(2)}$.

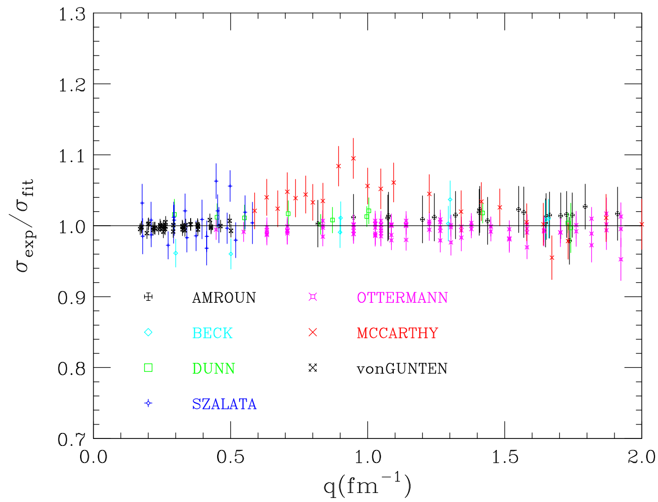

FIG. 2. (Color online) Ratio of experiment to fit for ^{3}He. Data with $\delta\sigma/\sigma > 0.1$ are not shown.

To determine the form factors, I have fitted the world data set, mainly in the form of unseparated cross sections, using the SOG parameterization for $G_e(q)$ and $G_m(q)$, thereby yielding the optimal e/m separation. The data were corrected for Coulomb distortion if this had not been already done by the authors. Random errors of the derived quantities were determined using the error matrix, the systematic errors of the data (mainly normalization) were included by changing the data sets by the quoted error, refitting and adding quadratically all the resulting changes. The SOG fit of the world data, comprising 354 data points up to $q_{\max} = 10$ fm^{-1}, has a χ^2 of 346. The results for the third Zemach moment and the rms radii are listed in Table II.

As for ^{4}He [6] the large-radius tail of the density has been constrained to have the fall-off as given by the proton separation energy (modulo corrections which are of minor quantitative impact). For the determination of the rms radius the knowledge on the large-r behavior of $\rho(r)$ is important to bridging the gap between the region of $0.5 < q < 1.2$ fm^{-1} where the data are sensitive to the rms radius to the $q = 0$ point where the rms radius is obtained from the slope of $G_e(q)$ as a function of q^2 [21]. Also for the Zemach moments the information on the large-r shape of $\rho(r)$ removes the major source of model dependence inherent in the choice of the parametrization for $\rho(r)$ or $G_e(q)$.

Contrary to the case of ^{4}He we do not know the absolute value of the density [6], so only the *shape* of $\rho(r)$ can be added as additional input. This shape is fitted for radii where the nucleon wave functions are in the asymptotic regime, i.e., where they are outside the nuclear potential and fall like a Whittaker function depending on the nucleon separation energy. This is the case for radii where the density typically has fallen to less than 1% of the density in the nuclear interior.

To explore a potential model dependence introduced by this procedure, I compared the radii determined using shapes from rather different sources. On the one hand side, I used the shapes from densities from Greens Function Monte Carlo [22] and Faddeev [23] calculations performed using modern $2N$ and $3N$ potentials. As an alternative, I calculated the p and n densities in a Woods-Saxon potential fitted to the form factor. The corresponding point densities were folded with the nucleon densities and added. Also in this case, the large-r behavior is given entirely by the p- and n-separation energies, which are accurately known from experiment. The comparison of the resulting moments shows no significant dependence on the tail shape used.

For a spin-1/2 nucleus such as ^{3}He it is also of interest to compute the standard (first) Zemach moment which can be obtained from the form factors via

$$\langle r\rangle_{(2)} = -\frac{4}{\pi}\int_0^\infty [G_e(q)G_m(q) - 1]\,\frac{dq}{q^2},$$

where $G_m(q)$ is the magnetic form factor (normalized at $q = 0$ to 1). This moment is needed to compute the finite size effects in the hyperfine splitting in muonic atoms, a quantity also being measured by the CREMA Collaboration. One could naively have expected that the hyperfine splitting would basically depend on the magnetization density $\rho_m(r)$ alone. The actual situation is somewhat more complicated, because

TABLE I. Moments for ^{4}He.

$\langle r^3\rangle_{(2)}$	16.73 ± 0.10 fm^3
$\langle r^2\rangle^{1/2}$	1.681 ± 0.004 fm
$\langle r^4\rangle$	14.35 ± 0.11 fm^4

TABLE II. Moments for ^{3}He.

$\langle r\rangle_{(2)}$	2.528 ± 0.016 fm
$\langle r^3\rangle_{(2)}$	28.15 ± 0.70 fm^3
$\langle r^2_{ch}\rangle^{1/2}$	1.973 ± 0.014 fm
$\langle r^2_m\rangle^{1/2}$	1.976 ± 0.047 fm
$\langle r^4_{ch}\rangle$	32.9 ± 1.60 fm^4

the lepton wave function inside the nucleus is influenced by the distribution of the charge.

The results for ^{3}He are $\langle r\rangle_{(2)} = 2.528 \pm 0.016$ fm and $\langle r^3\rangle_{(2)} = 28.15 \pm 0.70$ fm^3. For Gaussian (exponential) densities, which are often used to estimate the Zemach moments, $\langle r^3\rangle_{(2)}$ with the rms radius R of the SOG fit would amount to 26.68(29.10) fm^3; and $\langle r\rangle_{(2)}$, with both radii set to the experimental charge radius, would amount to 2.570(2.492) fm.

IV. ISOTOPE SHIFT

From the charge radii of ^{3}He and ^{4}He listed above, I deduced an isotope shift ^{3}He-^{4}He of $\delta\langle r^2\rangle = 1.066 \pm 0.06$ fm^2. This shift can be compared to values in [24–27] determined in atomic (electronic) helium.

Shiner *et al.* measured the 2^3S_1-2^3P_0 transition in ^{3}He, and Van Rooij *et al.* observed the orthohelium-parahelium, doubly forbidden transition between the metastable 2^3S_1 and 2^1S_0 states in ^{3}He and ^{4}He. Cancio Pastor *et al.* measured seven allowed transitions between the 2^3S and 2^3P manifolds. These authors found 1.066 ± 0.004 [26], 1.028 ± 0.011, and 1.074 ± 0.003 fm^2, respectively; the reason for the differences of several standard deviations is presently not understood. The shift from electron scattering agrees, but is not precise enough to favor one or the other of the values from atomic helium.

ACKNOWLEDGMENT

The author thanks Dirk Trautmann for helpful discussions.

[1] A. Antognini *et al.*, Can. J. Phys. **89**, 47 (2011).
[2] J. L. Friar and I. Sick, Phys. Lett. B **579**, 285 (2004).
[3] J. L. Friar and I. Sick, Phys. Rev. A **72**, 040502 (2005).
[4] I. Sick, Prog. Part. Nucl. Phys. **67**, 473 (2012).
[5] R. Pohl, A. Antognini, F. Nez, F. D. Amaro, F. Biraben, J. M. R. Cardoso, D. A. Covita, A. Dax, S. Dhawan, L. M. P. Fernandes, A. Giesen, T. Rraf, T. W. Hänsch, P. Indelicato, L. Julien, C.-Y. Kao, P. Knowles, J. A. M. Lopes, E.-O. Le Bigot, Y-W. Liu, L. Ludhova, C. M. B. Monteiro, F. Mulhauser, T. Nebel, P. Rabinowitz, J. M. F. dos Santos, L. Schaller, K. Schuhmann, C. Schwob, T. Taqqu, J. F. C. A. Veloso, and F. Kottmann, Nature **466**, 213 (2010).
[6] I. Sick, Phys. Rev. C **77**, 041302 (2008).
[7] R. Frosch, J. S. McCarthy, R. E. Rand, and M. R. Yearian, Phys. Rev. **160**, 874 (1967).
[8] U. Erich, H. Frank, D. Haas, and H. Prange, Z. Phys. **209**, 208 (1968).
[9] J. S. McCarthy, I. Sick, and R. R. Whitney, Phys. Rev. C **15**, 1396 (1977).
[10] R. G. Arnold, B. T. Chertok, S. Rock, W. P. Schütz, Z. M. Szalata, D. Day, J. S. McCarthy, F. Martin, B. A. Mecking, I. Sick, and G. Tamas, Phys. Rev. Lett. **40**, 1429 (1978).
[11] A. von Gunten, Ph.D. thesis, TH Darmstadt, 1982.
[12] C. R. Ottermann, G. Koebschall, K. Maurer, K. Roehrich, Ch. Schmitt, and V. H. Walther, Nucl. Phys. A **436**, 688 (1985).
[13] A. Camsonne *et al.*, Phys. Rev. Lett. **112**, 132503 (2014).
[14] Z. M. Szalata, J. M. Finn, J. Flanz, F. J. Kline, G. A. Peterson, J. W. Lightbody, Jr., X. K. Maruyama, and S. Penner, Phys. Rev. C **15**, 1200 (1977).
[15] P. C. Dunn, S. B. Kowalski, F. N. Rad, C. P. Sargent, W. E. Turchinetz, R. Goloskie, and D. P. Saylor, Phys. Rev. C **27**, 71 (1983).
[16] J. S. McCarthy, I. Sick, R. R. Whitney, and M. R. Yearian, Phys. Rev. Lett. **25**, 884 (1970).
[17] J. M. Cavedon, B. Frois, D. Goutte, M. Huet, Ph. Leconte, C. N. Papanicolas, X.-H. Phan, S. K. Platchkov, S. Williamson, W. Boeglin, and I. Sick, Phys. Rev. Lett. **49**, 978 (1982).
[18] I. Nakagawa, J. Shaw, S. Churchwell, X. Jiang, B. Asavapibhop, M. C. Berisso, P. E. Bosted, K. Burchesky, F. Casagrande, A. Cichocki, R. S. Hicks, A. Hotta, T. Kobayashi, R. A. Miskimen, G. A. Peterson, S. E. Rock, T. Suda, T. Tamae, W. Turchinetz, and K. Wang, Phys. Rev. Lett. **86**, 5446 (2001).
[19] H. Collard, R. Hofstadter, E. B. Hughes, A. Johanson, M. R. Yearian, R. B. Day, and R. T. Wagner, Phys. Rev. **138**, B57 (1965).
[20] D. Beck *et al.*, Phys. Rev. Lett. **59**, 1537 (1987).
[21] I. Sick and D. Trautmann, Phys. Rev. C **89**, 012201(R) (2014).
[22] I. Brida, S. C. Pieper, and R. B. Wiringa, Phys. Rev. C **84**, 024319 (2011).
[23] P. U. Sauer (private communication, 2000).
[24] R. van Rooij, J. S. Borbely, J. Simoneet, M. D. Hoogerland, K. S. E. Eikerma, R. A. Rozendaal, and W. Wassen, Science **333**, 196 (2011).
[25] P. Cancio Pastor, L. Consolino, G. Giusfredi, P. DeNatale, M. Inguscio, V. A. Yerokhin, and K. Pachucki, Phys. Rev. Lett. **108**, 143001 (2012).
[26] K. Pachucki, V. A. Yerokhin, and P. Cancio Pastor, Phys. Rev. A **85**, 042517 (2012).
[27] D. Shiner, R. Dixson, and V. Vedantham, Phys. Rev. Lett. **74**, 3553 (1995).